Phase separation during freezing upon warming of aqueous solutions

A. Bogdan[1,2,3,a)] and T. Loerting[1]

[1]*Institute of Physical Chemistry, University of Innsbruck, Innrain 80/82, A-6020 Innsbruck, Austria*
[2]*Laboratory of Polymer Chemistry, Department of Chemistry, University of Helsinki, P.O. Box 55, FIN-00014 Helsinki, Finland*
[3]*Department of Physical Sciences, University of Helsinki, P.O. Box 64, FI-00014 Helsinki, Finland*

Using differential scanning calorimetry, we show that the addition of solute(s) to emulsified water lowers the freezing temperature to <231 K, the homogeneous nucleation temperature of pure bulk water, or even completely suppresses freezing. In the latter case, freezing upon warming occurs above $T_X \approx 150$ K and leads to a phase separation into pure ice and a freeze-concentrated solution (FCS) which crystallizes upon further warming. We also show that emulsified 20–21.5 wt. % HCl solutions and the FCS of HCl/H$_2$O solutions transform to glass at $T_g \approx 127$–128 K, i.e., lower than $T_g \approx 136$ K of water. We suggest that water nanodrops adsorbed on fumed silica resemble bulk water more than water confined in nanoscaled confinement and also more than nanoscaled water domains in aqueous solution. © 2014 Author(s). All article content, except where otherwise noted, is licensed under a Creative Commons Attribution 3.0 Unported License. [http://dx.doi.org/10.1063/1.4898379]

INTRODUCTION

In the "no-man's land" (NML), which is the temperature region between homogeneous ice nucleation at $T_H \approx 231$ K and crystallization of a highly viscous liquid to cubic ice at $T_X \approx 150$ K, experiments on bulk water cannot be performed at atmospheric pressure because of rapid freezing.[1–5] The properties of supercooled water in this domain have remained speculative, therefore. These speculative issues include (i) the apparent singular temperature $T_s \approx 228$ K,[1,4,6] at which thermodynamic response functions (isothermal compressibility, K_T, isobaric heat capacity, C_P, and thermal expansion coefficient, α_P) were suggested to show a power-low divergence and hence to represent the spinodal temperature at ambient pressure, (ii) the position of the Widom lines (loci in the T-P diagram along which the response functions of K_T, C_P, and α_P attain their respective maximum values[7]), (iii) the hypothesized liquid-liquid separation[7] and (iv) the fragile-to-strong dynamic crossover.[8–10]

Water in the NML is usually investigated by computer simulations[2,11,13] and measurements of water confined in cylindrical nanopores of silica glasses,[1,3,9,10,14,15] see Fig. 1(a). We emphasize that, strictly speaking, the NML is defined for pure, bulk water, but not for water in solutions or water in confinement. The dynamic properties of freeze-concentrated solution (FCS or "water confined within ice itself"[16]), which was formed after freezing upon warming of quenched bulk TEMPOL/water solution, was studied with electron spin resonance spectroscopy.[17] It was concluded that the mobility of TEMPOL molecules in FCS was consistent with key issues concerning the properties of supercooled water in the NML.[17] It was also concluded by temperature-programmed desorption measurements on thin amorphous water films that they may crystallize above pure, bulk water's

crystallization temperature T_X.[18] However, the structure and dynamics of water layers adjacent to pore walls are drastically altered.[19–21] Strong and highly directional hydrogen bonds between SiOH and H$_2$O form a viscous boundary region up to 3 monolayers (∼0.9 nm) in which hydrogen bonding is strongly perturbed. At present, a large number of studies on confined water is undertaken using a wide range of substrates to assess the perturbation of structure and dynamics of bulk water by the confining walls.[12–15]

Other ways of lowering the freezing point to <231 K are the addition of solute(s) to water with subsequent emulsification[5] or the use of water nanodrops with a large free surface, for example, by the adsorption of vapour on fumed silica,[22,23] as schematically is shown in Fig. 1(b). In the past, experiments performed on emulsified sulphuric acid solutions showed that freezing and crystallization of ice could be avoided during a slow cooling/warming cycle.[5] Experiments performed on water nanodrops adsorbed on fumed silica showed that the freezing temperature may shift to below 228 K.[22] Recently, ultrafast X-ray measurements showed that some fraction of droplets cooled evaporatively remained liquid at 227 K on the time scale of milliseconds.[24] These authors employed micron-sized droplets, which are *per se* much closer to bulk water than the nanoscopic volumes of water studied by us here.

In this work, we show that emulsified solutions may or may not freeze at <231 K both upon cooling and warming. We also show to our best knowledge for the first time that: (i) freezing upon warming leads to a separation into pure ice and freeze-concentrated solution (FCS) and a second freezing event upon warming, (ii) the FCS of emulsified HCl/H$_2$O and emulsified ∼20–21.5 wt. % HCl solutions undergo a glass transition at $T_g \approx 127$ and 128 K, respectively, that is below $T_g \approx 136$ K of water. Analyzing published data, we propose that water nanodrops adsorbed on fumed silica resemble bulk water more than water confined

a)E-mail: anatoli.bogdan@uibk.ac.at
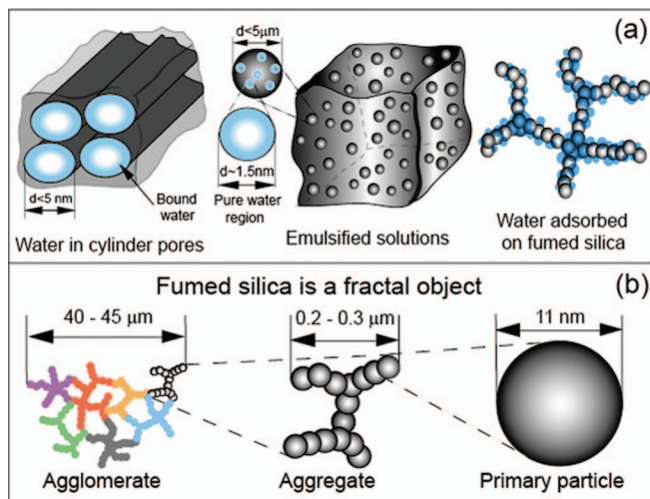
FIG. 1. Scheme of differently confined water. (a) Water in cylindrical nanopores, pure water regions in emulsified solutions drops, and water nanodrops obtained by the adsorption of vapour on fumed silica. (b) Fumed silica is a fractal object which forms a voluminous powder in which silica particles occupy less than 1% of total volume.

FIG. 2. Cooling (upper blue lines) and warming thermograms obtained from emulsified HNO_3/H_2O and $HNO_3/H_2SO_4/H_2O$. Thermograms (1) were obtained from 30 wt. % HNO_3, thermograms (2) from 32.5/1 wt. % HNO_3/H_2SO_4 which is the eutectic composition of 32.5 wt. % HNO_3 + 1 wt. % H_2SO_4, and thermograms (3) from 32.5/4 wt. % HNO_3/H_2SO_4. Freezing of ice, FCS, and solid mixture of ice/NAT/SAT are marked by $T_{f,ice}$, $T_{f,FCS}$, and $T_{f,mix}$, respectively. The melting of ice, NAT, SAT, eutectic ice/NAT, and ice/NAT/SAT are marked by $T_{m,ice}$, $T_{m,NAT}$, $T_{m,SAT}$, $T_{e,ice/NAT}$, and $T_{e,ice/NAT/SAT}$, respectively. T_g marks the onset of a liquid-to-glass and reverse glass-to-liquid transitions which are usually separated by ∼3K. Horizontal arrows mark the direction of temperature change. The scale bars denote heat flow through samples.

in nanopores or water in aqueous solutions. This is especially valid also at subzero temperatures. In aqueous solutions, some solutes such as ethanol suppress the anomalies of water in the supercooled state even at quite low mole fractions of 5%.[25]

EXPERIMENTAL

We prepared ∼30/0, 32.5/1, and 32.5/4 wt. % HNO_3/H_2SO_4 and ∼17, 20, and 21.5 wt. % HCl solutions by mixing ∼95–97 wt. % H_2SO_4, ∼65 wt. % HNO_3, and ∼37 wt. % HCl with the corresponding amount of ultrapure water. Water-in-oil and solution-in-oil emulsions were prepared using a widely used emulsification technique.[5,26] The diameter of drops in emulsions was <5 μm. We measured single half-sphere bulk water drops (4–6 mg) and emulsion samples (20–30 mg) with a Perkin-Elmer DSC-7 and Mettler Toledo DSC 822 calorimeters at cooling/warming rates of 3–5 K/min between 298 and 124 K.

RESULTS

In Fig. 2, we present thermograms obtained from emulsified solutions. In 30 wt. % HNO_3 (thermograms (1)), the freezing of ice at $T_{f,ice} \approx 167$ K is followed by a subtle transformation of FCS to glass with the onset at $T_g \approx 155$ K. Upon subsequent warming the reverse glass-to-liquid transition at $T_g \approx 152$ K and freezing of FCS at $T_{f,FCS} \approx 165$ K are observed. Upon further warming two endothermic events are seen, which we assign to the eutectic melting of ice/NAT (nitric acid trihydrate, $HNO_3 \cdot 3H_2O$, at $T_{e,ice/NAT} \approx 232$ K) and to ice melting (small peak at $T_{m,ice} \approx 237$ K). In the ternary solution of eutectic composition 32.5/1 wt. % HNO_3/H_2SO_4 (thermograms (2)), no freezing occurs upon cooling but only a liquid-to-glass transition at $T_g \approx 144$ K. Upon warming first the glass-to-liquid transition is observed at $T_g \approx 141$ K,

subsequently ice crystallizes at $T_{f,ice} \approx 156$ K and then the formed FCS freezes at $T_{f,FCS} \approx 166$ K to produce NAT and SAT (sulphuric acid tetrahydrate, $H_2SO_4 \cdot 4H_2O$). Upon further warming only eutectic melting of ice/NAT/SAT occurs at $T_{e,ice/NAT/SAT} \approx 231$ K.[26,27] In 32.5/4 wt. % HNO_3/H_2SO_4 (thermograms (3)) also only a liquid-to-glass transition occurs at $T_g \approx 145$ K. However, upon warming above $T_g \approx 142$ K, a single prolonged freezing process between ∼195 and 217 K produces a solid mixture of ice, NAT and SAT. Upon further warming the eutectic melting of ice/NAT/SAT is shifted by H_2SO_4 to $T_{e,ice/NAT/SAT} \approx 229$ K. The origin of the next melting double-peak is not clear. It could be produced by melting NAT and SAT.

Figure 3 displays the thermograms of emulsified HCl/H_2O. In 17 wt. % HCl/H_2O (thermograms (1)), the freezing of ice at $T_{f,ice} \approx 174$ K is followed by a liquid-to-glass transition of FCS (onset is hard to determine because of the inclined baseline). In the warming thermogram, a reverse glass-to-liquid transition at $T_g \approx 127$ K is observed. This is 9 K below water's $T_g \approx 136$ K. More precisely, it is 9 K below the calorimetric glass transition of low-density water, but 11 K above the calorimetric glass transition of high-density water.[28] The nature of the second glass transition at $T_g \approx 132$ K is not clear. In the past, a T_g of 126–130 K (also below water's T_g) was found for solutions of 2–3 mol. % of ethanol, ethylene glycol, and LiCl.[29]

The freezing of FCS at $T_{f,FCS} \approx 162$ K is followed by two eutectic melting events of ice/HAT (HCl trihydrate, $HCl \cdot 3H_2O$), $T_{ice,HAT} \approx 186$ K, and ice/HAH (HCl
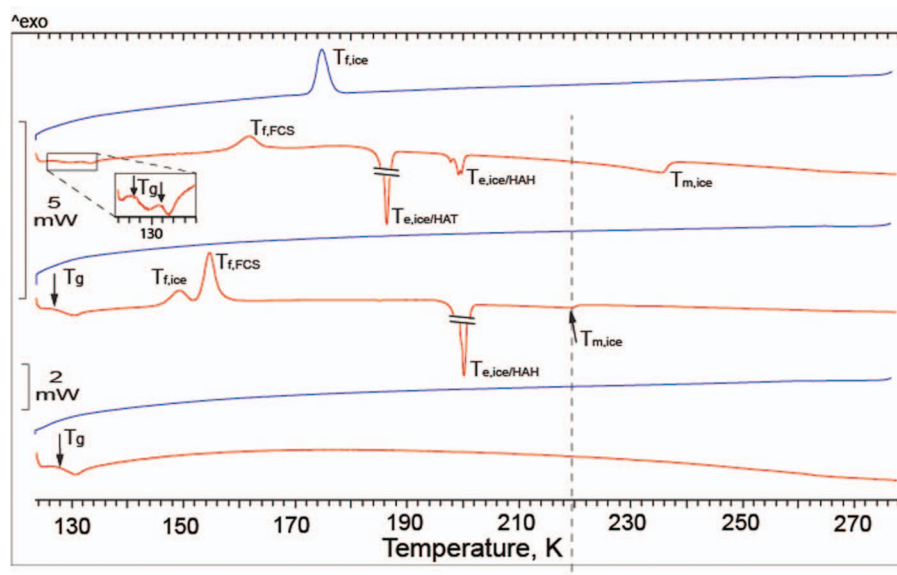
FIG. 3. Calorimetric thermograms of emulsified HCl/H$_2$O. Thermograms (1) were obtained from 17 wt. % HCl/H$_2$O, thermograms (2) from 20 wt. % HCl/H$_2$O, and thermograms (3) from 21.5 wt. % HCl/H$_2$O. $T_{ice,HAT}$ and $T_{ice,HAH}$ mark the eutectic melting of ice/HAT and ice/HAH. The last symbols are the same as in Fig. 2. The skewed line cuts transition peaks to fit the figure.

hexahydrate, HCl · 6H$_2$O), $T_{ice,HAH} \approx 200$ K and ice melting at $T_{m,ice} \approx 236$ K. In 20 wt. % HCl/H$_2$O (thermograms (2)), there are no freezing events but a liquid-to-glass transition which is also hard to determine. In contrast to 17 wt. % HCl, upon warming only one glass-to-liquid transition is seen at $T_g \approx 127$ K which is followed by ice freezing at $T_{f,ice} \approx 149$ K and the freezing of FCS at $T_{f,FCS} \approx 155$ K. Upon further warming, an eutectic melting occurs at $T_{ice,HAH} \approx 200$ K and ice melting at $T_{m,ice} \approx 220$ K. The melting of ice/HAT is absent. Finally, in 21.5 wt. % HCl/H$_2$O (thermograms (3)), there are no freezing and melting events but only the glass transition at $T_g \approx 128$ K.

Figures 2 and 3 demonstrate that phase separation into pure ice and FCS occurs both when freezing occurs upon cooling[5] and when crystallization of the devitrified solution occurs upon warming above T_g. As temperature decreases, the concentration inhomogeneity in liquid drops increases, i.e., solutions continuously fluctuate into pure water domains and regions of increasing concentration. In moderately concentrated solutions, the water/solute(s) ratio is relatively large and the size of pure water regions is ∼1.5 nm or larger.[5] Ice nucleation in the largest region may trigger freezing of a drop both upon cooling or warming. That is, in these solutions the interaction with the solute causes the patches of water to freeze below the homogeneous nucleation temperature of pure bulk water upon cooling and to freeze above the crystallization temperature of ultraviscous pure bulk water upon heating.

It was assumed that if solutions separate into pure ice and FCS during freezing then the low-temperature behaviour of such solutions could be similar to that of water.[5] If this is the case, then hydrogen bonding between H$_2$O in solutions and pure water could not differ strongly and, consequently, emulsified solutions may be used for the study of supercooled water in the NML. This suggestion finds a strong confirma-

tion in the above mentioned electron spin resonance measurements of FCS in frozen bulk TEMPOL/water solution.[18] However, no doubt that water hydrogen binding in solutions is perturbed, for example, by hydration shells. But how much the perturbations in solutions differ from those produced by pore walls remains an open question.

Figure 4 shows a comparison of the freezing behaviour for different types of water. Bulk water freezes rapidly at $T_{f,ice}$ and ice starts melting at ∼273 K, i.e., the calorimeter is well calibrated (thermograms (1)). The freezing of emulsified pure water drops occupies a large temperature region (thermograms (2)) and continues below $T_s \approx 228$ K. The double $T_{f,ice}$ is due to the bimodal size-distribution of drops. Nanodrops with a large free surface freeze at temperatures colder than emulsified drops and the freezing continues to ∼215 K (thermograms (3)).[22] Ice melting occurs between ∼236 and 264 K, i.e., ice crystals are very small and have a broad size-distribution. The average diameter of ice crystals was calculated using the Gibbs-Thomson equation and was found to be 7.6 nm.[22] The fact that water in pores of 3.43 nm in diameter freezes at temperatures warmer than the $T_{f,ice}$ of larger water samples suggests that it freezes heterogeneously (thermogram (4) vs. thermograms ((2) and (3)). Water nanodrops with a large free surface freeze at temperatures comparable or colder than that of water in nanopores (thermograms (3) vs. ((4) and (5)). It is unclear what the internal pressure of such adsorbed nanodroplets is, but according to the Young-Laplace equation it might be high, and so the droplets might resemble bulk water at higher pressures. Also, the surface to volume ratio in nanodrops is high, such that nanodrops might be representative of the surface structure of water. However, the absence of confining walls and long lifetime of nanodrops[22] makes them more suitable for a comparison with bulk water than water confined in nanoporous media.
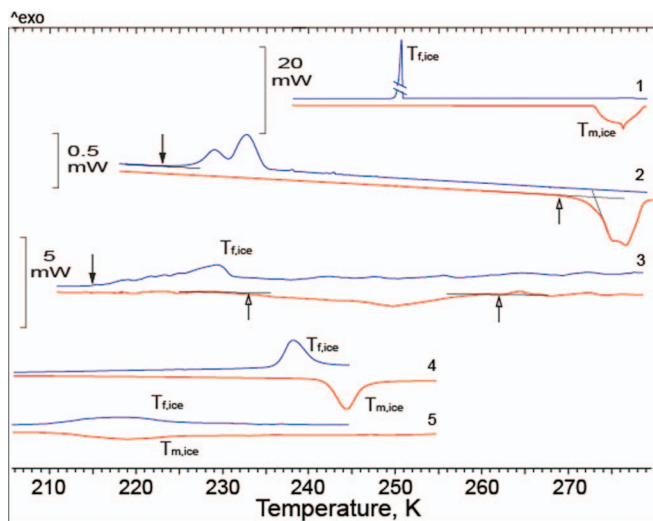
FIG. 4. Comparison of thermograms obtained from bulk water, emulsified water, nanodrops on fumed silica and water loaded in cylindrical nanopores. The thermograms (1) are obtained from a half-sphere drop (5.78 mg), thermograms (2) from emulsified water drops, thermograms (3) from water nanodrops with a large free surface of total weight of 1.7 mg,[22] and thermograms ((4) and (5)) from water loaded into cylindrical nanopores of diameter 3.43 and 3.03 nm.[30] The filled arrows mark the end of freezing and open arrows the beginning and end of ice melting. The thermograms (1) were obtained using a Mettler Toledo DSC 822, (2) Perkin-Elmer DSC-7 at 5 K/min, (3) Mettler DSC-30 at 3 K/min,[22] and ((4) and (5)) TA Instruments Model Q1000 DSC at 0.5 K/min.[30]

CONCLUSIONS

Our calorimetric measurements show that liquid water may be studied in aqueous solution below 231 K and above 150 K. Water nanodrops adsorbed on fumed silica, emulsified aqueous solutions near the eutectic composition or water confined in nanometer-sized pores may be used to that end. Whether or not such studies may help in understanding bulk water needs to be addressed in future studies. We propose that water nanodrops adsorbed on fumed silica may show the least perturbation compared to bulk water and may be most relevant for our understanding of the properties of supercooled water.

[1]J. Swenson and J. Teixeira, J. Chem. Phys. **132**, 014508 (2010).
[2]E. B. Moore and V. Molinero, J. Chem. Phys. **132**, 244504 (2010).
[3]F. Mallamace *et al.*, Proc. Natl. Acad. Sci. U.S.A. **104**, 424 (2007).
[4]P. G. Debenedetti and H. E. Stanley, Phys. Today **56**, 40 (2003).
[5]A. Bogdan, J. Phys. Chem. **110**, 12205 (2006).
[6]R. J. Speedy and C. A. Angell, J. Chem. Phys. **65**, 851 (1976).
[7]F. Mallamace, C. Corsaro, and H. E. Stanley, Proc. Natl. Acad. Sci. U.S.A. **110**, 4899 (2013).
[8]K. Ito, C. T. Moynihan, and C. A. Angell, Nature (London) **398**, 492 (1999).
[9]L. Liu, S. H. Chen, A. Faraone, C. W. Yen, and C. Y. Mou, Phys. Rev. Lett. **95**, 117802 (2005).
[10]F. Mallamace *et al.*, J. Chem. Phys. **124**, 161102 (2006).
[11]E. B. Moore, E. de la Llave, K. Welke, D. A. Scherlis and V. Molinero, Phys. Chem. Chem. Phys. **12**, 4124 (2010).
[12]N. Giovambattista, P. J. Rossky, and P. G. Debenedetti, Phys. Rev. E **73**, 041604 (2006).
[13]N. Giovambattista, P. G. Debenedetti, and P. J. Rossky, J. Phys. Chem. C **111**, 1323 (2007).
[14]E. Tombari, G. Salvetti and G. P. Johari, J. Phys. Chem. C **116**, 2702 (2012).
[15]E. Tombari and G. P. Johari, J. Chem. Phys. **139**, 064507 (2013).
[16]F. Mallamace, Proc. Natl. Acad. Sci. U.S.A. **106**, 15097 (2009).
[17]D. Banerjee, S. N. Bhat, S. V. Bhat and D. Leporini, Proc. Natl. Acad. Sci. U.S.A. **106**, 11448 (2009).
[18]R. S. Smith and B. D. Kay, Nature (London) **398**, 788 (1999).
[19]R. K. Iler, *The Chemistry of Silica* (Wiley, New York, 1978), Chaps. 5 and 6.
[20]D. R. Bassett, E. A. Boucher, and A. C. Zettlemoyer, J. Colloid Interface Sci. **34**, 436 (1970).
[21]D. R. Bassett, E. A. Boucher, and A. C. Zettlemoyer, J. Colloid Interface Sci. **27**, 649 (1968).
[22]A. Bogdan, M. Kulmala, and N. Avramenko, Phys. Rev. Lett. **81**, 1042 (1998).
[23]A. Bogdan, M. J. Molina, M. Kulmala, A. R. MacKenzie, and A. Laaksonen, J. Geophys. Res. **108**(D10), 4302 doi:10.1029/2002JD002605 (2003).
[24]J. A. Sellberg *et al.*, Nature (London) **510**, 381 (2014).
[25]O. Conde, J. Teixeira, and P. Papon, J. Chem. Phys. **76**, 3747 (1982).
[26]A. Bogdan, M. J. Molina, H. Tenhu, E. Mayer, and T. Loerting, Nat. Chem. **2**, 197 (2010).
[27]K. D. Beyer, A. R. Hansen, and N. Raddatz, J. Phys. Chem. A **108**, 770 (2004);
[28]K. Amann-Winkel *et al.*, Proc. Natl. Acad. Sci. U.S.A. **110**, 17720 (2013).
[29]K. Hofer, A. Hallbrucker, E. Mayer and G. P. Johari, J. Phys. Chem. **93**, 4674 (1989).
[30]S. Jähnert, F. V. Chavez, G. E. Schaumann, A. Schreiber, M. Schönholf, and G. H. Findenegg, Phys. Chem. Chem. Phys. **10**, 6039 (2008).